Phys. Status Solidi B **252**, No. 1, 87–94 (2015) / **DOI** 10.1002/pssb.201350398

Part of Topical Section on
Optics of Surfaces and Interfaces

physica status solidi b
www.pss-b.com
basic solid state physics

Early oxidation stages of the strained Ge/Si(105) surface: A reflectance anisotropy spectroscopy study

Claudio Goletti*[,1], Laura Fazi[1], Conor Hogan[2,3], Luca Persichetti[1,†], Anna Sgarlata[1], Maurizia Palummo[3], and Adalberto Balzarotti[1]

[1] Dipartimento di Fisica and CNISM, Università degli Studi di Roma "Tor Vergata", Via della Ricerca Scientifica 1, 00133 Roma, Italy
[2] Istituto di Struttura della Materia, Consiglio Nazionale delle Ricerche (CNR-ISM), Via del Fosso del Cavaliere 100, 00133 Roma, Italy
[3] Department of Physics and European Theoretical Spectroscopy Facility (ETSF), Università degli Studi di Roma "Tor Vergata", Via della Ricerca Scientifica 1, 00133 Roma, Italy

Received 16 December 2013, revised 17 March 2014, accepted 18 March 2014
Published online 2 May 2014

Keywords density functional theory, oxidation, reflectance anisotropy spectroscopy, vicinal silicon surfaces

* Corresponding author: e-mail goletti@roma2.infn.it, Phone: +39 06 72594288, Fax: +39 06 2023507
† Current address: Department of Materials, ETH Zurich, Wolfgang-Pauli-Strasse 10, 8093 Zurich, Switzerland.

We have applied reflectance anisotropy spectroscopy (RAS) to investigate the rebonded-step (RS) reconstructed strained Ge/Si(105) surface. RAS spectra display a marked peak at 2.1 eV that is completely cancelled after exposure to about 1200 L of molecular oxygen. *Ab initio* calculations of the RAS signal explain the experimental spectra in terms of optical transitions between filled bulk-like states and empty surface bands. The early stages of exposure of the clean surface to molecular oxygen have been monitored by RAS and scanning tunneling microscopy (STM), correlating the evolution of the optical anisotropy to the bonding configuration of the adsorbed gas. Oxygen atoms are proposed to first adsorb onto the arms and later on the head dimers of the "horseshoe" motifs that comprise the RS reconstruction, thus gradually destroying the local order.

1 Introduction Although the golden age of surface physics dates back to the 1980s and 1990s, a true surface-science approach is still being followed to study the clean surface properties of materials technologically important for electronics [1], magnetism [2], photovoltaic devices [3], organic film growth [4], as well as to solve puzzling and significant scientific issues still not understood [5]. Within this evergreen scientific interest, optical spectroscopies – mainly reflectance anisotropy spectroscopy (RAS) [6] and surface differential reflectance (SDR) [7] – assume a special role because they combine the nondestructive character of light with high surface sensitivity, thus becoming a powerful tool to investigate clean semiconductor [8, 9] and metal surfaces [10, 11] as well as more complex interfaces and systems [12]. A very significant contribution is also provided by theory that is now able to simulate optical spectra in impressive agreement with experimental results [5, 13]. In addition, RAS can be easily coupled to other surface sensitive techniques (such as scanning tunneling microscopy [STM]) that enhance its capabilities, as well as to complex experimental apparatuses (e.g., molecular beam epitaxy [MBE]) [14].

In this paper, we use RAS to investigate the Ge-terminated silicon surface, nominally Ge/Si(105), obtained by evaporating Ge onto a particular vicinal Si(001) surface, close to the (105) plane. This surface exhibits a complex reconstruction of the top layer, where Ge atoms are arranged in a regular pattern of "horseshoe" motifs. The rebonded step model, hereafter referred to as rebonded-step (RS), is shown in Fig. 1 [15]. It is well known that the RS reconstruction has been identified on the {105} facets of the Ge and SiGe pyramidal islands grown onto Si(001) surfaces after deposition and annealing of germanium [16]. Until now, this surface structure has been characterized mainly by STM [17] and atomic force microscopy (AFM) [18], but a true spectroscopic study is still lacking, as the size of facets is much reduced (a few tens of square nanometers) with respect to the typical dimensions of optical and electronic probes. Recently, however, it has been shown that a whole RS-reconstructed surface layer is obtained after annealing of a

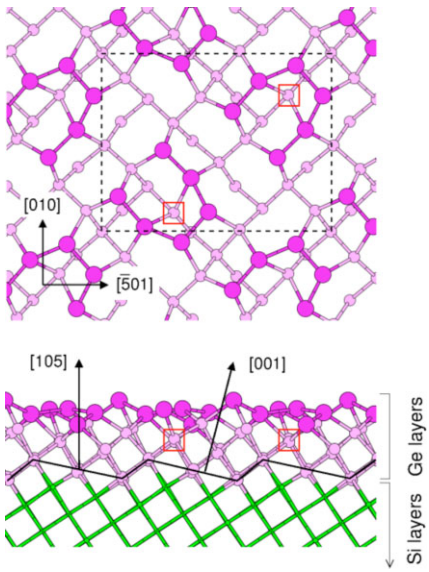

Figure 1 Schematic structure of the Ge/Si(105) rebonded-step surface reconstruction after 4 ML Ge coverage (above: top view; below: side view). Pink circles represent Ge atoms, while subsurface Si layers are shown in green. In the unit cell (dashed box), interstitial Ge atoms are highlighted (see text). An abrupt interface between Ge layers and Si bulk has been assumed here. For a more detailed discussion, see Ref. [20].

Ge-terminated silicon vicinal surface with miscut angle $\theta = 11.5^\circ$ toward the [100] direction [19], thus permitting new optical investigations [20].

The utility of RAS to investigate this surface is clearly substantiated by the electronic anisotropy displayed in STM pictures of the RS surface (Fig. 2), which shows an almost unidimensional chain-like pattern along the [$\bar{5}$01] direction. This symmetry is not evident in the structural model of the surface due to the considerable relaxation and rebonding across the S_A- and S_B-type steps in the unit cell (Fig. 1).

The experimental optical spectra are interpreted in terms of transitions involving surface states that are characteristic of the RS reconstructed surface, through a close comparison with theoretical curves computed within density functional theory and an independent particle approach to the optical response (DFT-IP). With respect to ref. [20], particular attention has been given to the variation of the optical response of the clean surface during exposure to molecular oxygen. This offers a decisive demonstration of the surface character of the detected anisotropies. In addition, the early stages of the oxidation process are investigated, and a possible route for the oxygen adsorption is proposed, via a comparison of RAS data with images taken with STM.

The results reported here are also valuable for gaining a better knowledge of oxidation at germanium surfaces. This is an important but poorly understood technological aspect that limits the development and the application of germanium-based devices [21].

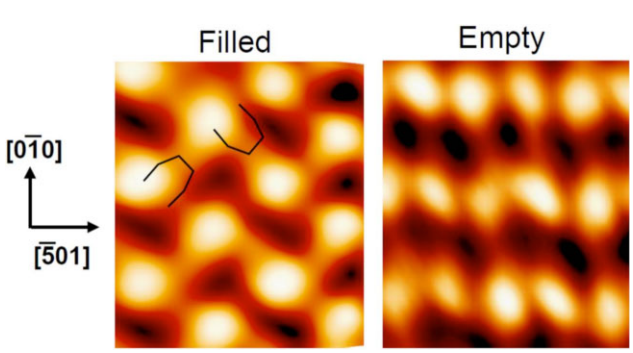

Figure 2 Experimental STM image ($4.2 \times 4.2\,\mathrm{nm}^2$) of a RS reconstructed Ge/Si(105) surface. Both filled ($V = -1.5$ V; $I = 1.5$ nA) and empty states ($V = +1.0$ V; $I = 0.7$ nA) are reported. A sketch of the horseshoe motif of the reconstruction is indicated. The chain-like atomic pattern runs along the [$\bar{5}$01] direction.

2 Experimental and calculations

2.1 RAS and STM experiments Experiments were carried out in an ultrahigh-vacuum chamber ($p < 4 \times 10^{-11}$ mbar) equipped with an Omicron STM and a RAS spectrometer, on vicinal Si(001) wafers miscut by 11.5° toward the [100] direction. The RS-reconstruction was prepared through physical vapor deposition of Ge at room temperature followed by annealing at about 870 K. The deposition rate was 0.3 ML min^{-1}. STM and RAS experiments have been conducted with the sample at room temperature.

A compact home-made RAS apparatus has been used in the version with two polarizers [22], to perform measurements in the 1.5–5.0 eV range. Normal-incidence optical access to the sample was obtained by a UHV quartz strain-free window that introduces a negligible background anisotropy in the whole photon energy range.

The results are given in terms of the ratio between the difference ΔR of the intensity of reflected light (polarized alternately along directions α and β of the substrate) and the average value $R = (R_\alpha + R_\beta)/2$, as a function of the photon energy:

$$\frac{\Delta R}{R} = \frac{2(R_\alpha - R_\beta)}{R_\alpha - R_\beta}. \quad (1)$$

In the present case, the directions α and β lie along [$\bar{5}$01] and [0$\bar{1}$0] of the clean surface, respectively, parallel and perpendicular to the zig-zag rows of atoms visible in Fig. 2 (or equivalently, to the offcut/step direction).

To eliminate spurious contributions from the optical setup, the residual anisotropy of the oxidized surface ($\Delta R/R^{\mathrm{oxid}}$) has been subtracted from each experimental curve. All the data are thus presented as $\Delta\mathrm{RAS} = \Delta R/R - \Delta R/R^{\mathrm{oxid}}$.

2.2 Oxidation High-purity molecular oxygen has been introduced in the UHV chamber by a leak valve, at a pressure lower than 1×10^{-7} torr. The O_2 partial pressure was continuously controlled by a quadrupole mass spectrometer. Two different oxidation experiments have

been conducted: (a) experiment #1: on two halves of the same sample, RAS and STM experiments were performed *simultaneously*, and the RAS signal variation in time at fixed photon energy was followed while the surface was exposed to gas at partial pressure p; (b) experiment #2: the inlet of oxygen was interrupted at defined exposure stages, and each time a complete RAS spectrum was acquired in the range 1.8–3.0 eV, and STM images were recorded. After each stage of experiment #2, the leak valve was opened again to introduce oxygen, and so on. In this case, the RAS signal has also been monitored during exposure.

Each $\Delta R/R$ value has been measured at a certain exposure. All the oxidation experiments were conducted at room temperature.

2.3 DFT-LDA calculations Calculations were carried out from first principles using density functional theory in the local density approximation (DFT-LDA) [23]. A plane wave basis set was used, with kinetic energy cut-off of 30 Ry, and norm-conserving, scalar relativistic pseudopotentials [24]. Nonlinear core corrections were used for Ge [25]. Structural relaxations and calculations of electronic occupied and unoccupied eigenstates were performed using the PWscf code, part of the quantum-ESPRESSO suite [26].

Surfaces were modeled using supercells containing 22 Å thick nonsymmetric slabs separated by vacuum regions about 14 Å thick. The lattice constant of bulk silicon, 5.40 Å, was adopted in order to replicate the conditions of strain felt by the Ge adlayer. Dangling bonds at the bottom of the slab were terminated with hydrogen, and several back layers of Si were kept fixed at the bulk positions during structural relaxation. The remaining atoms were relaxed until individual force components were less than 12 meV $Å^{-1}$. A $(2 \times 2 \times 1)$ k-point mesh was used for surface Brillouin zone (SBZ) sampling.

Optical spectra were computed at the independent particle level through calculation of the slab dielectric tensor [27] using the Yambo code [28]. Dense $(8 \times 8 \times 1)$ k-point meshes yielded well-converged spectra below 5 eV. The optical response from the passivated side of the slab was removed using a real space cut-off technique [29]. To account for the underestimation of the bandgap within DFT-LDA, we applied a scissors operator [30] of +0.4 eV estimated from the difference between the experimental E_2 critical point energy (~4.25 eV) and the computed value (~3.85 eV). Thus, we approximately account for many-body, size quantization and finite-temperature effects in the computed spectra.

Structural models adopted for the H-passivated and oxygen-covered RS-reconstructed surfaces will be discussed in Section 4.2.

3 Results ΔRAS spectra of the clean and RS reconstructed Ge-terminated (105) surface are shown in Fig. 3. In STM images, clean Si(105) appears atomically rough, and does not exhibit any reconstruction or long-range order (Fig. 4, panel a). In the corresponding RAS curve, a nearly null signal (apart from a weak oscillation) is measured below 3 eV, while at higher photon energy an almost linear decrease of the anisotropy is recorded.

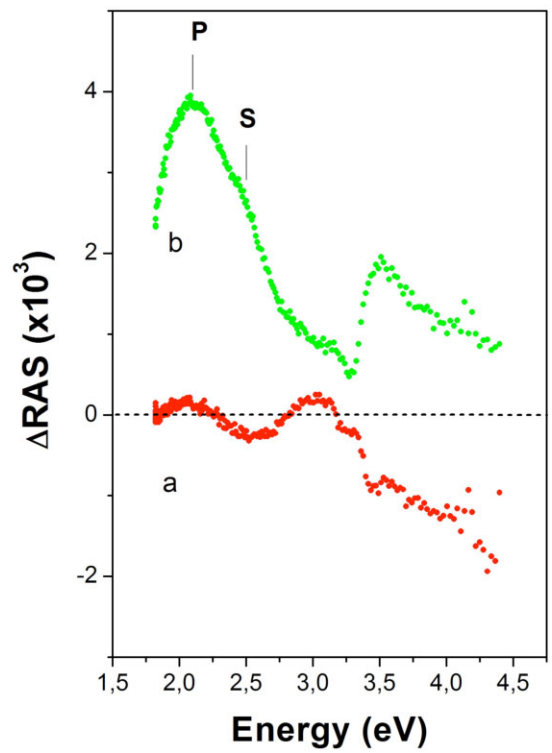

Figure 3 Experimental ΔRAS spectra for the clean Si(105) surface (lower, in red) and after growth of 4 ML of germanium (upper, in green). In all the reported curves, the residual optical anisotropy $\Delta R/R^{oxid}$ (measured on the fully oxidized surface) has been subtracted.

After deposition of 4 ML of Ge and subsequent annealing, the RS reconstruction forms across the whole surface (as demonstrated by STM: see Fig. 4, panel b). In the low-energy region of the spectrum, an evident anisotropic peak (P) develops, having a maximum at 2.1 eV, along with an additional shoulder (S) at about 2.5 eV. Above 3 eV, where the bulk critical points of silicon lie, RAS detects a structure around 3.4 eV.

When the RS reconstructed surface is exposed to molecular oxygen, the 2.1 eV peak is progressively washed out, and disappears completely above 1140 L (Fig. 5). STM images taken during the same experiment (see below) demonstrate that the attenuation of the optical signal and the progressive disappearance of the RS reconstruction are thoroughly intertwined. The ΔRAS variations monitored in both cases (experiment #1 and experiment #2) are nearly coincident (Fig. 5), substantiating that the effect of gas chemisorption does not depend upon the different details of the oxidation in our experiments. Some kinetic effects (that at this level we cannot better define) are possible, to explain the little discrepancies between the two curves. Within this

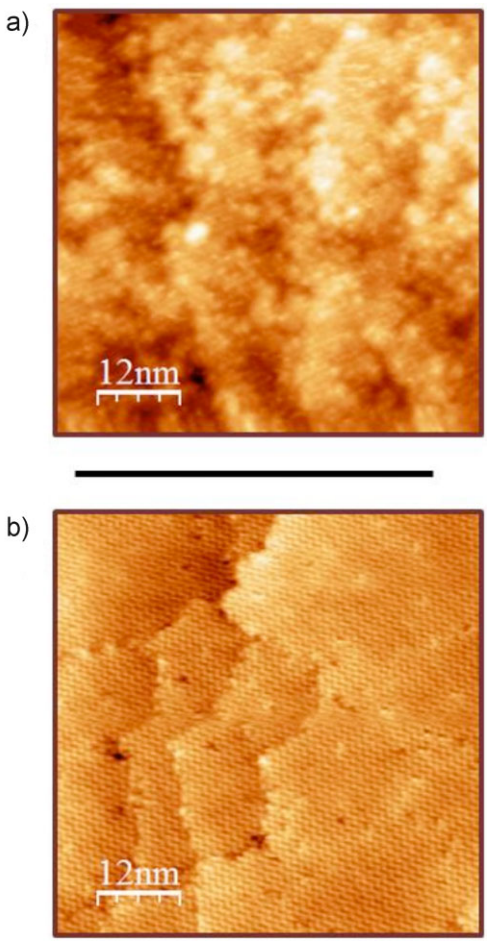

Figure 4 STM images of the Si(105) surface (panel a, $61 \times 61\,\mathrm{nm}^2$; $V = -1.2\,\mathrm{V}$, $I = 1.15\,\mathrm{nA}$), and of the reconstructed Ge/Si(105) surface (panel b, $61 \times 61\,\mathrm{nm}^2$; $V = -1.5\,\mathrm{V}$, $I = 0.5\,\mathrm{nA}$). The zig-zag pattern of the RS reconstruction (with chains running along the $[\bar{5}01]$ direction) is visible in panel b.

approximation, STM images acquired during experiment #1 can be referred to the ΔRAS spectra measured at the same exposure value during experiment #2 (and vice versa), thus relating structural information with the modifications of the electronic bands.

The RAS spectra acquired at increasing oxidation stages are plotted in Fig. 6, showing the evolution of the main peak P during exposure: in particular, the peak position and the lineshape are almost unmodified, indicating that the oxidation process apparently affects this anisotropy feature as a whole.

4 Discussion

4.1 RAS spectra: Experiment and theory The ΔRAS spectrum of the clean Si(105) surface (Fig. 3) is essentially structureless below 3 eV: as negligible contributions from bulk silicon electronic states are expected in this energy range [8], we conclude that no surface-related anisotropies are detected. From STM inspection, the clean

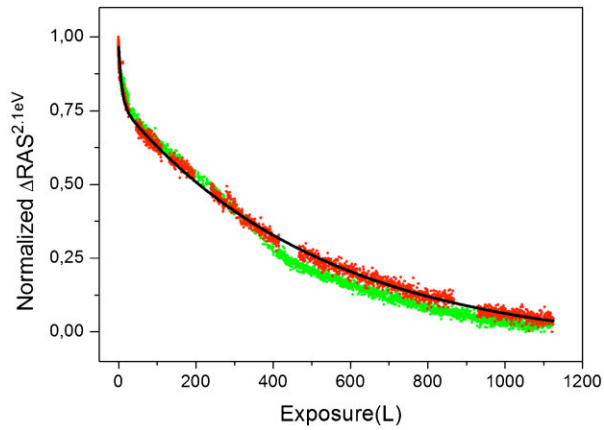

Figure 5 ΔRAS signal (measured at 2.1 eV, the maximum anisotropy signal in Fig. 3) versus exposure to molecular oxygen, expressed in Langmuir (1 Langmuir $= 1 \times 10^{-6}$ torr s). Differently colored curves refer to different oxidation experiments (green: experiment #1; red: experiment #2. See text for details). For each experiment, the signals have been normalized to the corresponding maximum. The black curve is the fit of data for experiment #2 by means of the sum of two Langmuir functions, describing the adsorption on two different sites, with different sticking coefficients (see text).

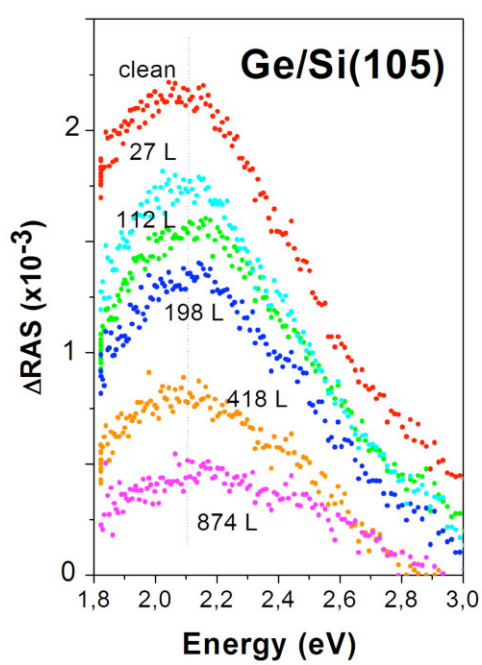

Figure 6 Experimental ΔRAS spectra for the Ge/Si(105) surface at successive steps of oxidation (values in Langmuir are reported). In all the curves, the residual optical anisotropy $\Delta R/R^{\mathrm{oxid}}$ (measured at the fully oxidized surface, after 1140 L) has been subtracted. By definition, ΔRAS spectrum at 1140 L is thus zero everywhere (the related curve is not reported). The amplitude of P for the clean surface is sample dependent: thus in this experiment we have measured about 2.2×10^{-3}, at variance with the spectrum shown in Fig. 3, reporting a higher value.

surface appears disordered and rough with a roughness in the range 5–8 Å (Fig. 4a). At this miscut value, the resulting mean terrace width is not large enough to contain a unit cell of the clean 2×1 dimer reconstructed surface and thus the surface does not show any reconstruction or order [19]. The negative ΔRAS signal, decreasing almost linearly at photon energies higher than 3 eV could be due in part to surface roughness [31–33].

The ΔRAS spectrum of the RS-reconstructed surface, obtained after Ge deposition and annealing, appears completely different, mainly through the occurrence of the peak P, apparently as a consequence of the Ge termination of the surface (Fig. 3). The true surface origin of P rests on two strong arguments: (i) below 3 eV, no contributions from bulk silicon anisotropies are expected [7, 8]; (ii) the peak P is sensitive to oxygen exposure (Figs. 5 and 6), and vanishes at about 1140 L, a value consistent with the oxidation of surface states in Ge and Si [34, 35]. Confirmation of the surface origin of P and S features in the clean Ge/Si(105) optical response comes from theoretical calculations of the RAS spectra, which allow us to single out the states involved in transitions. The DFT-IP calculations are in excellent agreement with experiment, as shown in Fig. 7.

In order to provide an appropriate comparison with the experimental curves, theoretical spectra have been plotted both as $\Delta R/R$ and as a difference with respect to the H-covered surface (thus mimicking ΔRAS curves). Some disagreement with experiment is perceptible in the high-energy region, as one could expect, since the bulk contributes differently to the curves in the two cases [36]. The contribution from the topmost (Ge) layers is also shown, confirming the localized surface origin of the low-energy peaks.

The interpretation of the two main anisotropy structures is the following: peak P is due to electronic transitions from filled bulk states to an empty state associated with the backbond of the "interstitial" atom highlighted in the red box in Fig. 1 (hereafter indicated in the text as *i*), which exhibits the characteristic of a true surface state. Shoulder S is due to transitions from bulk bands to the empty surface state of the top dimer at the apex of the horseshoe motif.

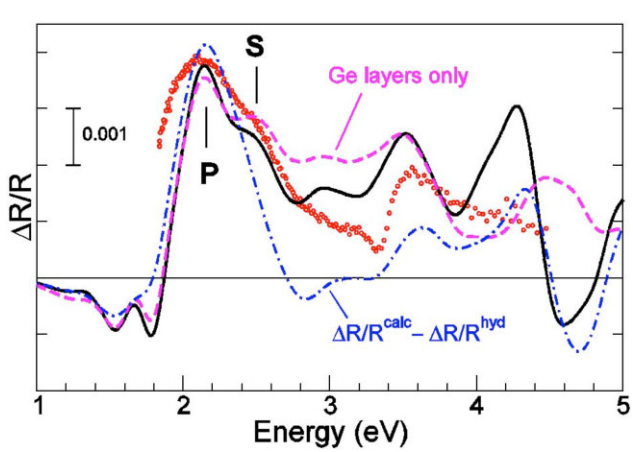

Figure 7 Calculated $\Delta R/R$ (solid line, black) and ΔRAS (dot-dashed line, blue) spectra of the Ge/Si(105) RS reconstructed surface, for a 4 ML coverage of Ge, compared with the experimental ΔRAS signal (dots, red). The contribution from the Ge layers only is also shown (dashed line, violet).

The peculiar origin of the interstitial state explains the unusual dependence of the peak P intensity upon Ge coverage, reported and discussed exhaustively in Ref. [20], and allows extraction from RAS data information about the composition of the subsurface region that is not accessible with STM or other surface-sensitive techniques. On the contrary, RAS is able to reach and investigate the buried interface between silicon and germanium. In our calculations, such an interface is assumed to be sharp, although some degree of intermixing could be still consistent with results [20].

4.2 Oxidation The intensity decrease of peak P (Fig. 5) is due to the gradual chemisorption of oxygen, which by establishing new bonds with Ge atoms at the surface removes the associated optical transitions [34, 35]. The experimental curve, reflecting the oxidation kinetics, does not follow a simple Langmuir behavior [37], in contrast with the cleavage surface of Si and Ge, where a stick-or-leave model with one adsorption site is able to explain the optical data at room temperature [34, 35]. On the contrary, a more complex dependence upon exposure occurs in Fig. 5. Three different steps can be singled out in the process: (i) step #1 (below 5 L, 1 Langmuir $= 1 \times 10^{-6}$ torr s), where the sticking coefficient S (associated to the curve slope) reaches the highest value; (ii) step #2 (5–500 L), with a lower and nearly constant value of S; (iii) step #3 (above 500 L), which continues until the signal saturates to zero at about 1140 L. The fit with two Langmuirian curves (black line in Fig. 5) is in reasonable agreement with the experiment: this means that two different adsorption sites are very likely to occur, with different initial sticking coefficients ($S_1 \sim 0.12$, $S_2 \sim 0.0019$), as well as with different surface densities (about 1:4). Given the different dependences of two processes upon exposure ($S_1 \gg S_2$), their sum produces three steps in the resulting curves: (i) step 1: the fast process (S_1) dominates; (ii) step 2: both processes display comparable effects; and (iii) step 3: the slow process (S_2) prevails.

The Langmuirian curves are related to the presence of two different and independent adsorption sites on the surface (e.g., dangling bonds and backbonds). However the origin and the role of these sites, as well as their related densities, will be not discussed here, but developed in a later study on a detailed STM investigation of the oxidation process of Ge/Si(105) surfaces.

In Fig. 6, experimental ΔRAS spectra are shown for the Ge/Si(105) surface at successive steps of oxidation. In the clean surface curve, the shoulder S is not clearly visible, but appears more distinctly at higher exposure values. This is the effect of a sample dependence of the P and S features, the latter expressing a strong dependence upon the long range

order of the reconstructed layer: the more extended the surface order of the RS phase, the higher is the resulting S amplitude.

ΔRAS curves in Fig. 6 do not exhibit a significant lineshape variation upon exposure of the corresponding relic anisotropy spectrum: the effect of adsorption in removing the electronic states that contribute to the optical anisotropy is nearly the same across the whole photon energy range. Nevertheless, a small decrease in the ratio I_P/I_S (I_P and I_S being the RAS intensities at the P and S photon energies, respectively) is perceptible during exposure, thus indicating a weak preferential adsorption. Although the ΔRAS spectra exhibit a slight blueshift with increasing exposure, we determined that the distinct optical components giving rise to P and S do not change (to within ±20 meV) [38]. The curve width weakly reduces: the higher disorder of the oxidizing surface has apparently no strong effect in the optical curve.

For the RS reconstructed Ge/Si(105), P is connected with the interstitial atom *i*, in its turn linked to dimers at the surface (thus contributing also to the S amplitude): on the basis of RAS data, it is thus difficult to select the surface sites where atoms (or molecules) preferentially stick, in contrast to the case of oxygen and hydrogen on Si(100)2 × 1 [39–41]. In those experiments, optical data and theoretical calculations explain the oxidation data well: thanks to the remarkable site dependence of optical structures, adsorption of oxygen atoms has been assigned first to backbonds and later to dangling bonds of the clean Si(100) surface, the former more reactive than the latter.

Can an oxidation route be inferred also here on a speculative basis? In Fig. 8, some models are shown for the oxygen layer adsorbed onto clean Ge/Si(105), under the hypothesis that gas molecules dissociate on the surface [42–44]. In each case, we assumed that the Ge overlayer forms a sharp interface with the Si substrate (see Fig. 1). Elsewhere, we have demonstrated that a rough interface does not greatly modify the RAS response [20]. For H-passivation we considered the simplest model that saturates surface dangling bonds (Fig. 8, panel b); hence, surface dimers are retained. Oxidation is more difficult to model, due to the presence of various chemisorption processes, several competing adsorption sites, energy barriers and kinetic effects. Studies of the Ge(100) surface, which also features surface Ge dimers, act as a guide [42–45]. At low coverages, DFT calculations predict that oxygen molecules dissociate and adsorb at single dimers, inserting into (or on top of) dimers and backbonds [41]; at intermediate coverages Ge substitution and dimer breaking is reported [43, 44]. We consider separately the case of oxygen adsorption at the "arms" of the horseshoe only [model (I), Fig. 8 panel c], and following additional adsorption at the "head" dimer [model (II), Fig. 8 panel d]. These two models will allow us to identify the distinct optical response of the two kinds of adsorption site. To understand the exposure dependence, oxidation (I) and oxidation (II) can be also interpreted as possible stages of the same chemisorption process.

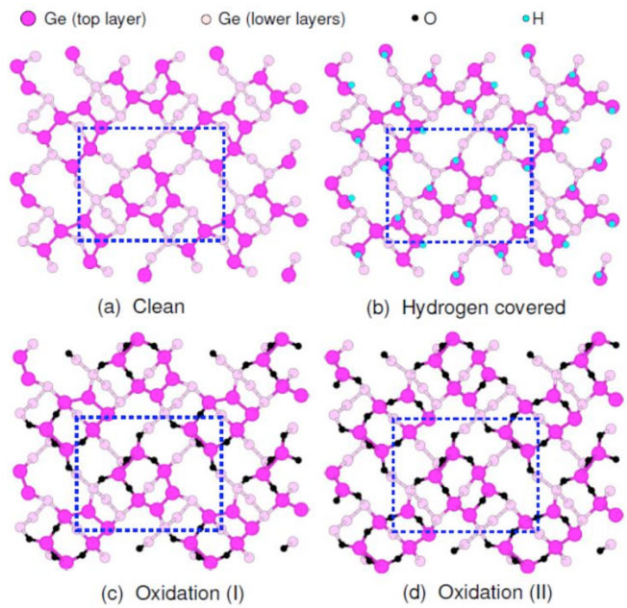

Figure 8 Schematic models of: (a) the "clean" Ge/Si(105) surface at 4 ML of Ge (Ge atoms of the first layer are shown as large pink circles, deeper layers have a lighter color); (b) the same surface passivated with hydrogen; (c) and (d) the same surface after adsorption of oxygen [two different coverages; labeled as oxidation (I) and oxidation (II)]. The surface unit cell is indicated (dashed rectangle). Hydrogen and oxygen atoms have been reported as light-blue and black circles, respectively.

Although an exhaustive examination of the microscopic oxidation process is beyond the scope of this work, RAS calculations of the oxidized surfaces are in general agreement with our interpretation of the experimental behavior (Fig. 9). First, oxidation of the horseshoe arms, leaving the head dimers untouched [model (I)], produces a

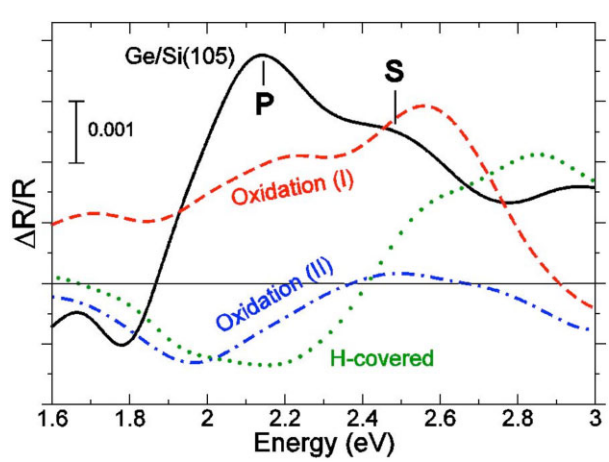

Figure 9 Calculated $\Delta R/R$ spectra around the main peak for the clean, H- and O-covered models of Ge/Si(105) shown in Fig. 7a. Models assumed for oxidation (I), oxidation (II) and the H-covered surface have been reported in Fig. 8.

40% reduction of peak P, while S is slightly shifted and enhanced. An exact comparison cannot be expected here due to the oxygen-related perturbations on the bulk-like states that take part in the optical transitions, and that are hard to quantify. Further oxidation also of the head dimer produces an overall quenching of both P and S. Due to the redistribution of charge among the different horseshoe dimers following oxygen absorption, as well as the unknown perturbation on the bulk-like states that also take part in the optical transitions, we feel it is premature, however, to speculate further about the relationship between oxidation site and RAS peak modification based only on these results: a more detailed interpretation is left to a later study.

The procedure of our experiments permits us to connect optical data with STM images, thus linking the electronic information coming from RAS to the structural details, in order to identify the bonding geometries resulting after oxidation. A complete and detailed analysis of STM images taken during oxidation will appear in the near future. In Fig. 10, we report a $50 \times 50\,\mathrm{nm}^2$ area of the sample after nominal exposure to 5 L of oxygen, to represent a typical situation during oxidation. The RS reconstruction is visible across the whole area, as are defects due to oxygen adsorption. In the very early stages of oxidation (step #1), exposure to gas results in isolated protrusions on the surface (indicated by arrows in the figure), appearing as white, structureless dots (with a profile at about 1 Å above the surface layer). Other less bright dots, corresponding to a level in the range 0.2–0.5 Å above the surface, apparently can aggregate and evolve (step #1 and #2): somewhere they are organized in linear structures, like *fingers* in the direction [010], perpendicular to two or more adjacent chains (circles in Fig. 10); somewhere (more seldom) they disappear, possibly as a consequence of desorption or diffusion along the surface. As each STM image has been acquired in about 2 min, it is possible that we had not the necessary time resolution, and missed some details on that scale. The *fingers* themselves develop, increasing their length because of clustering. A third structure appears in images, often close to the *fingers*, in the form of dark regions, first isolated, then gathered in little islands (squares in the figure). From a line profile, these areas are apparently about 1 Å below the surface plane. Up to 500 L (step #2), both structures (*fingers* and dark spots, the latter dominant) are disseminated on the sample surface, progressively cancelling the RS reconstruction. Finally (step #3), the disorder of the layer increases until the surface appears completely rough, and any trace of reconstruction is washed out at about 1200 L. No 1×1 ordering is present.

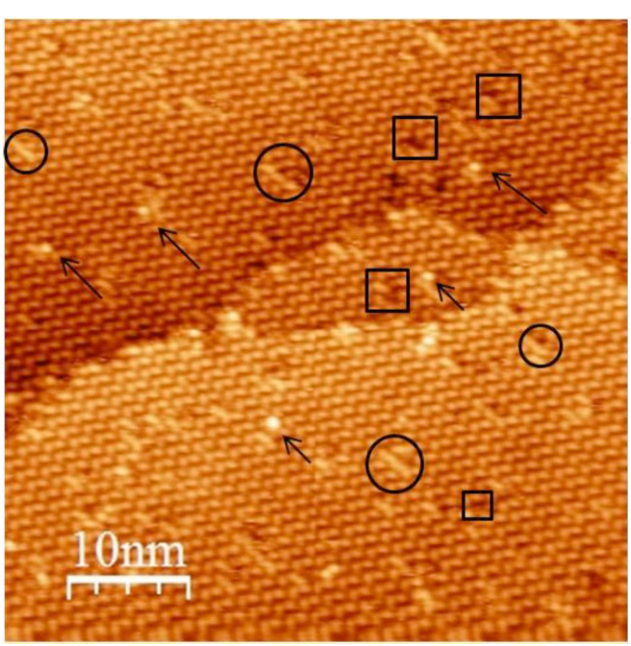

Figure 10 STM image ($50\,\mathrm{nm} \times 50\,\mathrm{nm}$, $V = -1.9\,\mathrm{V}$, $I = 0.900$ nA) of the Ge/Si(105) surface after exposure to 5 L of oxygen. The zig-zag pattern of the RS reconstruction is clearly visible (with chains running along the $[\bar{5}01]$ direction). The effects of oxidation have been highlighted: (i) protrusions (by arrows); (ii) fingers (by circles); and (iii) dark spots (by squares). For details, see the text.

The three types of surface sites determined by analysis of our STM images fit the nomenclature introduced to clarify the features seen in the STM pictures of Ge(001) oxidized surfaces [43]. The bright site – imaged at about 1 Å above the surface layer – could thus be a Ge adatom, (a residual of the surface preparation, or due to substitution with oxygen in a backbond [41]), or a single O atom/molecule adsorbed onto the surface. *Fingers* would come from coalescence of oxygen atoms: (i) adsorbed into backbonds, for example, at the interstitial atom *i*; or (ii) bonded to the dimers in the arms of the horseshoe, as suggested by the calculations above. In high-resolution images (not shown here), *fingers* appear due to lines of dots, each dot in correspondence of a corner of the RS zig-zag rows. The dark site, on the contrary, is normally localized where DFT simulations show arm dimer bonds [20]. We note that, although at a preliminary level, such a scenario is consistent with our conclusions from RAS data.

High-resolution STM experiments coupled with systematic modeling of the chemisorption process and DFT calculations of the STM images, will yield a more complete picture of the oxidation process. New optical experiments will be performed in order to probe the photon energy region down to at 1.3 eV, where the true surface-to-surface transitions are expected from calculations [20]. Experiments at different sample temperatures will help us to investigate the details of the oxidation kinetics (as in Ref. [34]).

Acknowledgements The authors dedicate this paper to the memory of Wolfgang Richter. We thank Massimo Fanfoni for useful discussions. C.H. and M.P. acknowledge high-performance supercomputing resources and support from CINECA through the ISCRA initiative. This work has been carried out as ETSF User Project No. 467. One of the authors (L.P.) acknowledges

Regione Lazio project GESTO. Finally, the technical contribution of personnel from our Department (M. Iannilli, G. Vitali, and D. Pecchi) has been very valuable for interfacing the RAS apparatus to the STM chamber.

References

[1] U. Diebold, Surf. Sci. Rep. **48**, 53 (2003).
[2] H. Brune and P. Gambardella, Surf. Sci. **603**, 1812 (2009).
[3] O. Bikondoa, C. L. Pang, R. Ithnin, C. A. Muryn, H. Onishi, and G. Thornton, Nature Mater. **5**, 189–192 (2006).
[4] L. D. Sun, J. Gall, G. Weidlinger, C. Y. Liu, M. Denk, and P. Zeppenfeld, Phys. Rev. Lett. **110**, 106101 (2013).
[5] G. Bussetti, B. Bonanni, S. Cirilli, A. Violante, M. Russo, C. Goletti, P. Chiaradia, O. Pulci, M. Palummo, R. Del Sole, P. Gargiani, M. G. Betti, C. Mariani, R. M. Feenstra, G. Meyer, and K. H. Rieder, Phys. Rev. Lett. **106**, 067601 (2011).
[6] P. Weightman, D. S. Martin, R. J. Cole, and T. Farrell, Rep. Prog. Phys. **68**, 1251 (2005).
[7] S. Selci, F. Ciccacci, G. Chiarotti, P. Chiaradia, and A. Cricenti, J. Vac. Sci. Technol. A **5**, 327 (1987).
[8] C. Goletti, F. Arciprete, S. Almaviva, P. Chiaradia, N. Esser, and W. Richter, Phys. Rev. B **64**, 193301 (2001).
[9] J. R. Power, P. Weightman, S. Bose, A. I. Shkrebtii, and R. Del Sole, Phys. Rev. Lett. **80**, 3133 (1998).
[10] D. S. Martin and P. Weightman, Surf. Interface Anal. **31**, 915 (2001).
[11] Ph. Hofmann, K. C. Rose, V. Fernandez, A. M. Bradshaw, and W. Richter, Phys. Rev. Lett. **75**, 2039 (1995).
[12] B. Sheridan, D. S. Martin, J. R. Power, S. D. Barrett, C. I. Smith, C. A. Lucas, R. J. Nichols, and P. Weightman, Phys. Rev. Lett. **85**, 4618 (2000).
[13] C. Hogan, E. Ferraro, N. McAlinden, and J. F. McGilp, Phys. Rev. Lett. **111**, 087401 (2013);
M. Palummo, N. Witkowski, O. Pluchery, R. Del Sole, and Y. Borensztein, Phys. Rev. B **79**, 035327 (2009);
S. Wall, B. Krenzer, S. Wippermann, S. Sanna, F. Klasing, A. Hanisch-Blicharski, M. Kammler, W. G. Schmidt, and M. Horn-von Hoegen, Phys. Rev. Lett. **109**, 186101 (2012).
[14] F. Arciprete, C. Goletti, E. Placidi, C. Hogan, P. Chiaradia, M. Fanfoni, F. Patella, and A. Balzarotti, Phys. Rev. B **69**, 081308 (2004).
[15] P. Raiteri, D. B. Migas, L. Miglio, A. Rastelli, and H. vonKanel, Phys. Rev. Lett. **88**, 256103 (2002).
[16] J. Tersoff, B. J. Spenser, A. Rastelli, and H. von Kanel, Phys. Rev. Lett. **89**, 196104 (2002).
[17] Y. Fujikawa, K. Akiyama, T. Nagao, T. Sakurai, M. G. Lagally, T. Hashimoto, Y. Morikawa, and K. Terakura, Phys. Rev. Lett. **88**, 176101 (2002).
[18] T. Eguchi, Y. Fujikawa, K. Akiyama, T. An, M. Ono, T. Hashimoto, Y. Morikawa, K. Terakura, T. Sakurai, M. G. Lagally, and Y. Hasegawa, Phys. Rev. Lett. **93**, 266102 (2004).
[19] L. Persichetti, A. Sgarlata, G. Mattoni, M. Fanfoni, and A. Balzarotti, Phys. Rev. B **85**, 195314 (2012).
[20] L. Fazi, C. Hogan, L. Persichetti, C. Goletti, A. Sgarlata, M. Palummo, and A. Balzarotti, Phys. Rev. B **88**, 195312 (2013).
[21] C. Claeys and E. Simoen, Germanium-Based Technologies: from Materials to Devices (Elsevier, Amsterdam 2007).
[22] A. Salvati and P. Chiaradia, Appl. Opt. **39**, 5820 (2000);
C. Goletti, G. Bussetti, P. Chiaradia, A. Sassella, and A. Borghesi, Org. Electron. **5**, 73 (2004).
[23] P. Hohenberg and W. Kohn, Phys. Rev. B **136**, 864 (1964);
W. Kohn and L. J. Sham, Phys. Rev. A **140**, 1133 (1965);
J. P. Perdew and A. Zunger, Phys. Rev. B **23**, 5048 (1981).
[24] N. Troullier and J. L. Martins, Phys. Rev. B **43**, 1993 (1991).
[25] S. G. Louie, S. Froyen, and M. L. Cohen, Phys. Rev. B **26**, 1738 (1982).
[26] P. Giannozzi, S. Baroni, N. Bonini, M. Calandra, R. Car, C. Cavazzoni, D. Ceresoli, G. L. Chiarotti, M. Cococcioni, I. Dabo, A. Dal Corso, S. Fabris, G. Fratesi, S. de Gironcoli, R. Gebauer, U. Gerstmann, C. Gougoussis, A. Kokalj, M. Lazzeri, L. Martin-Samos, N. Marzari, F. Mauri, R. Mazzarello, S. Paolini, A. Pasquarello, L. Paulatto, C. Sbraccia, S. Scandolo, G. Sclauzero, A. P. Seitsonen, A. Smogunov, P. Umari, and R. M. Wentzcovitch, J. Phys.: Condens. Matter **21**, 395502 (2009) and http://www.quantum-espresso.org.
[27] F. Bechstedt, Principles of Surface Physics (Springer-Verlag, Berlin, 2003).
[28] A. Marini, C. Hogan, M. Gruning, and D. Varsano, Comput. Phys. Commun. **180**, 1392 (2009) and online at http://www.yambo-code.org
[29] C. Hogan, R. Del Sole, and G. Onida, Phys. Rev. B **68**, 035405 (2003).
[30] R. Del Sole and R. Girlanda, Phys. Rev. B **48**, 11789 (1993).
[31] T. Yasuda, L. Mantese, U. Rossow, and D. E. Aspnes, Phys. Rev. Lett. **74**, 3431 (1995).
[32] D. E. Aspnes, Thin Solid Films **89**, 249 (1982).
[33] D. E. Aspnes, J. B. Theeten, and F. Hottier, Phys. Rev. B **20**, 3292 (1979).
[34] C. Goletti, P. Chiaradia, L. Moretti, W. Yian, G. Chiarotti, and S. Selci, Surf. Sci. **356**, 68 (1996).
[35] G. Chiarotti, P. Chiaradia, E. Faiella, and C. Goletti, Surf. Sci. **453**, 112 (2000).
[36] Long-range effects of band bending or strain variation due to annealing are not completely considered in the calculations.
[37] The classical Langmuir model describes the adsorption of a single species on a surface site. It is a stick-or-leave model: if the surface site is free, the species is adsorbed with a probability depending upon the sticking coefficient S; if it is occupied, the species goes back onto the gas phase. For a more detailed description see Ref. [34] and references therein.
[38] The presence, amplitude and width of P and S components contributing to the ΔRAS curves has been carefully evaluated after deconvolution of the imaginary part of the anisotropic surface dielectric function (within the three-layer model, see J. D. E. McIntyre, and D. E. Aspnes, Surf. Sci. **24**, 417 (1971)). For more details, see for example Ref. [8].
[39] O. Pluchery, N. Witkowski, and Y. Borensztein, Phys. Status Solidi B **242**, 2696 (2005).
[40] K. Gaál-Nagy, A. Incze, G. Onida, Y. Borensztein, N. Witkowski, O. Pluchery, F. Fuchs, F. Bechstedt, and R. Del Sole, Phys. Rev. B **79**, 045312 (2009).
[41] J. Takizawa, S. Ohno, J. Koizumi, K. Shudo, and M. Tanaka, J. Phys.: Condens. Matter **18**, L209 (2006).
[42] J. Soon, C. Lim, K. Loh, N. Ma, and P. Wu, Phys. Rev. B **72**, 115343 (2005).
[43] T. J. Grassman, S. R. Bishop, and A. C. Kummel, Surf. Sci. **602**, 2373 (2008).
[44] T. Fukuda and T. Ogino, Phys. Rev. B **56**, 13190–13193 (1997).
[45] C. Fleischmann, K. Schouteden, C. Merckling, S. Sioncke, M. Meuris, C. Van Haesendonck, K. Temst, and A. Vantomme, J. Phys. Chem. C **116**, 9925 (2012).